Virtual testing of a composite cylindrical lattice structure for aerospace applications

J. Torres[a], N. Blanco[a], E. Del Olmo[b], E. Grande[b]

[a] AMADE, Mechanical Engineering and Industrial Construction Department, Universitat de Girona, Campus Montilivi s/n, E-17071, Spain.

[b] EADS CASA Espacio, Avda. Aragón, 404 - E -28022 Madrid, Spain.

Composite lattice structures manufactured with Advanced Fiber Placement are a promising weight saving solution for replacing the current aluminum and traditional composite structures for aerospace applications. A virtual testing procedure for designing lattice structures using FE commercial program Abaqus v6.9 was developed and used to design a composite cylindrical lattice for aerospace applications. The virtual testing study was divided in two stages. First, a parametric analysis was used for choosing the most adequate configuration of the technology demonstrator. The second stage consisted in a detailed test simulation of the geometry of the specimen selected. A beam based model assessed the global structure response and a complete solid model combined with the submodeling technique was used to calculate the different failure indices: intralaminar failure was calculated with a user routine and adhesive peel-off was analyzed through a stress criterion, Virtual Crack Closure Technique (VCCT) and cohesive elements. The results of the virtual testing demonstrated a proper load capacity of the lattice specimen. These results are to be validated once the real specimen already manufactured has been tested.

Keywords: Aerospace, Composites, Lattice, Buckling, Frequency, Failure, Submodeling

1. Introduction

Grid composite structures are a promising solution for replacing some of the current aluminium and composite parts for aerospace applications. Composite materials are characterized by their great specific strength and stiffness along the fibre direction, while the mechanical properties in the other directions are not so favourable. Moreover, the use of the traditional composite laminates in the structural design does not make the most of the potential of composite materials. In contrast, the principal load-bearing elements in grid structures are unidirectional composite ribs, maximizing their specific structural contribution. Therefore, grid composite designs could represent a significant weight saving with respect to traditional composite laminates (Vasiliev, 2006). In addition, the manufacturing process of grid composite structures can be completely automated and it provides integral structures, since assembling operations can be eliminated. As a consequence, a significant cost saving can be achieved in the manufacturing process (Vasiliev, 2006). Other important advantages of grid composite structures are less sensitivity to imperfections and improved damage tolerance with respect to more traditional composite designs (Vasiliev, 2001).

In general, grid structures can be composed by a lattice pattern reinforcing one-side or both-sides shell structures or skins. Then, the structure is designated as a grid-stiffened structure while when it is formed only with the lattice pattern it is simply designated as a lattice structure. If the design of the lattice pattern follows a symmetrical and regular geometry with planar isotropic behavior the structure is known as isogrid. If the planar behavior of the lattice pattern cannot be considered isotropic, the structure is referred to as anisogrid. Although the skin contributes with some extra stability to the structure, its structural contribution is low while it significantly increases the total weight. Consequently, in the specific literature it is a common trend to dismiss the use of skins in this type of structures, especially when the optimization of grid composite structures in terms of weight is considered (Bunakov, 1999). Figure 1 shows a couple of examples representative of both designing approach: a grid-stiffened structure (A) and a lattice one (B). Both have been manufactured by EADS CASA Espacio (ECE) following composite layering method (Advance Fiber Placement, AFP) within the frame of the research Project call ICARO.

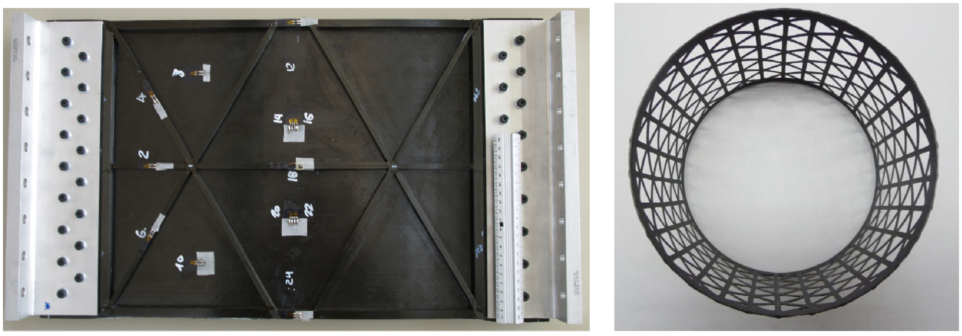

(a) (b)

Figure 1. Examples of grid-stiffened and lattice structures manufactured by EADS CASA Espacio following automatic layering method (Advance Fiber Placement). (a) Grid-stiffened structure. (b) Lattice structure.

The use of grid-stiffened composite structures for spacecraft load-carrying structures has been studied in Russia for the last fifteen years and different anisogrid conical and cylindrical structures have been designed and manufactured by means of the filament winding technique. (Vasiliev, 2001) proposed an analytical continuum model based on smeared stiffness for the general case of a cylindrical or conical grid-stiffened structure with helical and circumferential ribs, thin inner and outer skin and foam core. However, the formulation to predict critical loads associated to the main failure modes is only defined for lattice structures. Vasiliev and co-workers (Vasiliev, 2001; Vasiliev, 2006) reported the use of the constitutive equation of the smeared stiffness in combination with the Finite Element Method (FEM) in the analysis of lattice patterns. Morozov et al. (2011) analyzed the buckling behavior of anisogrid composite lattice cylinders with FEM completely modeled with beam elements.

The smeared stiffness approach has been recently compared to a finite element structural analysis of a quadrigrid plates under transverse loads determining that the smeared stiffness is useful for design optimization although an exact numerical model is required for the final designs (Cagdas, 2009). In the same direction, Moutain (2007) analyzed the use of anisogrid lattice structures as a replacement of skin-stringer wing covers for aeronautical applications and found an excellent agreement between an analytical model smearing the stiffness and an exact FE model. Vasiliev and co-workers (Vasiliev, 2006; Vasiliev 2007) also defined the optimal structural parameters for lattice cylinders subjected to axial compression. Based on these results, (Totaro, 2009) found an optimal design of a lattice cylinder using a MATLAB™ non-linear optimization algorithm with some simplifications on the design variables and failure constraints.

Novel composite manufacturing processes such as the AFP technique enhance the design and manufacturing of lattice and grid-stiffened composite structures. In fact, AFP allows the design of different tailored fiber directions while in filament winding composite tows must follow the geodesic path. Indeed, AFP was used for the fabrication of an entire advanced grid-stiffened structure for the Minotaur payload fairing (Wegner, 2002; Higgins, 2002; Higgins, 2004; Higgins, 2005). The design and testing procedures, from material characterization to full-size test, were reported for a low load demanding structure such as the Minotaur payload fairing.

The concept of virtual testing was developed for the design and structural assessment using numerical simulations not only as a tool but as the central core of the process. Virtual testing is not simply a structural and stress analysis, it is a complete prediction of the behavior of the material, component and structure including all possible failure mechanisms. In this way, the industry can reduce time and resource consuming experimental test campaigns by trustable numerical simulations (Davies, 2008). Virtual testing is a promising technique for structural analysis allowing a reduction in design time, cost of certification and facilitating optimization (Llorca, 2009). There are two possible approaches for virtual testing: bottom-up and top-down models (Cox, 2006). The bottom-up method consists on simulating the failure of the analyzed element by building up detailed models of molecular processes and applying them to the entire structures. Actually, it can be seen as a multi-scale analysis involves micro and macro models that can be costly in computational terms. On the other hand, the top-down method begins with a relatively coarse structural analysis, which is progressively refined by incorporating the necessary details.

This paper presents the modeling work carried out to build a virtual testing tool with capacity to support iterations on the design tasks associated to the evaluation of a new structural concept based on lattice approach for aerospace applications. The tool developed has been implemented with the commercial program Abaqus/Standard v6.9. The validation of the computational results will be done on a cylindrical lattice tested under compression load. This full size structural technology demonstrator has been manufactured by ECE following AFP manufacturing methods. It is a very well consolidate technology at EADS CASA Espacio and has been selected to build a new generation of ultralight structured based on both grid and lattice design. As described in (Vasiliev, 2001), the test campaign involved a full-size demonstrator to consider the AFP fabrication parameters that depend on the specimen size and which cannot be correctly considered with the test of small-size specimens.

2. Virtual testing procedure

In order to assist the design of a cylindrical lattice composite structure for aerospace applications a tool based on a virtual testing procedure was implemented with the commercial program Abaqus v6.9. The virtual testing procedure presented in this paper corresponds to a top-down method (Cox, 2006) in which a full-size technology demonstrator was designed and simulated.

The procedure followed for developing the virtual testing tool was implemented in different steps, which are summarised in Figure 2. First, a parametric analysis with a preliminary model was carried out in order to determine the best design solution for the cylindrical lattice structure. Due to the nature of lattice structures, the geometry of all the lattice configurations was completely parameterized and analysed with beam type element simulations. The results of the parametric analysis represented a useful decision tool for helping in the selection of the best possible design of the structure.

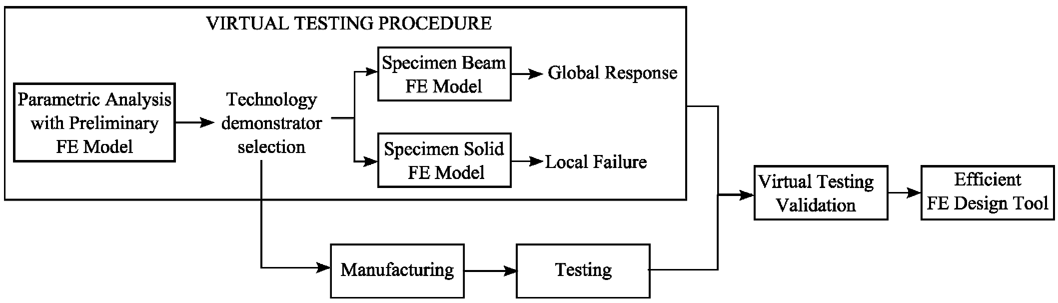

Figure 2. Procedure for developing a virtual testing tool.

The second part of virtual testing consisted in a testing simulation of the full-size lattice technology demonstrator. As a consequence of the size differences between the large-scale structure and the local interactions, the virtual testing was divided in two analyses. A FE model composed basically with beam elements assessed the global structural response. The local failure information was obtained with a FE model only including solid elements.

Finally, results obtained with the virtual testing procedure must be compared and validated with experimental results. The final objective is developing a prediction tool with a reduced cost iteration process in the design of new space lattice structures.

These steps and the details of the FE models used in each case are further explained in the following section.

3. FE model definition

1. Virtual testing – Part 1: Selection of technology demonstrator

As mentioned before, the full-size technology demonstrator considered for the development of the virtual testing procedure was a composite cylindrical lattice structure for aerospace applications. This simply geometry was chosen instead of more complicated ones, such as conical geometries, because it is a common a geometry for aerospace structures, it is relatively easy to manufacture (specially when compared to conical geometries) and numerical and experimental can be more easily interpreted and understood. Moreover, cylindrical geometries are more conservative than conical geometries in terms of strength and there are analytical models (Vasiliev, 2001) whose predictions can be compared to the numerical and experimental results.

The base material considered in the FE analysis was a prepreg tape of epoxy matrix reinforced with unidirectional carbon fibers Epoxy/M40J manufactured by Toray with a nominal layer thickness of 0.14 mm. The material elastic properties considered in the present study are summarized in Table 1.

Table 1. Epoxy/M40J/ UD CFRP elastic material properties.

E_{11} (MPa)	$E_{22} = E_{33}$ (MPa)	$\upsilon_{12} = \upsilon_{13}$	υ_{23}	$G_{12} = G_{13}$ (MPa)	G_{23} (MPa)
199000	7800	0.3	0.5	3860	2600

A preliminary model with a completely parameterized geometry was created for a parametric analysis. The model was formed only with beam elements *B31*. An example of a simple cylinder in lattice configuration is shown in Figure 3. The dimensions proposed in this first design stage are also included in Figure 3 although these were only approximate and were changed in the final stages of the design process. The load introduction interfaces were not modeled with the objective to only study the most efficient lattice configuration and simplify the analysis. Also with the aim of simplicity, the geometry of the ribs was assumed to be perfectly rectangular and all rib intersections were supposed ideal (coinciding three ribs in a point as shown in Figure 3).

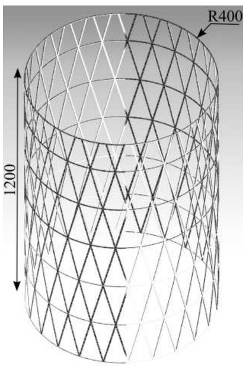

Figure 3. Geometry of a lattice cylinder configuration modeled with beam elements for the parametric analysis (Dimensions in mm).

The design variables considered in the parametric analysis were the number of helical and circumferential ribs and the rib thickness. The width of the ribs, both helical and circumferential, was fixed to the width of two fiber tows. A total of 120 cases were modeled with the combination of the design variables shown in Table 2. The angle of the helical ribs with respect to the circumferential ribs varied for each configuration as a result of the variation of the number of helical ribs.

Table 2. Design variables used in the parametric analysis

Design Variable	Min. Value	Max. Value	Increments	no. Cases
no. helical ribs	24	40	4	5
no. circumferential ribs	6	16	2	6
Rib thickness [mm]	4	7	1	4
			Total	120

The parametric study consisted in a frequency analysis, a buckling analysis to ensure that the considered configuration met the natural frequencies and buckling load requirements and a gravity step in order to calculate the associated mass. Although the chosen technology demonstrator was a cylinder, the frequency analysis specifications were adapted from a conical structure of the VEGA launcher (ICARO project team, 2010) and are summarized in Table 3. In the buckling analysis the equivalent load calculated from the accelerations suffered from the launcher during the flight was applied as a pure compression load F = 259 kN in upper extreme of the structure. In the frequency and buckling analysis the lower extreme was clamped (U1 = U2 = U3 = UR1 = UR2 = UR3 = 0) and coupling constraints were applied between of the nodes in the upper extreme and the mass point located in the Spacecraft (S/C). CoG is the distance between the upper extreme of the specimen and the mass point.

Table 3. Frequency analysis specifications (S/C stands for Spacecraft) (ECE).

S/C Mass [kg]	S/C CoG [mm]	S/C Ixx [kg·m^2]	S/C Iyy,Izz [kg·m^2]
2000	2000	1400	3000

The results of the parametric analysis relating each lattice configuration with its response in terms of natural frequencies, buckling load and mass were analyzed and used for the selection of the best lattice configuration for the technology demonstrator. A cylindrical lattice configuration formed by 36 helical ribs and 14 circumferential ribs with a fixed thickness of 6 mm in both cases was chosen as the most appropriate.

2. Virtual testing – Part 2: Test simulation

As mentioned, after the parametric analysis carried out in the first stage of the process, a cylindrical lattice configuration with 36 helical ribs and 14 circumferential ribs was selected. The thickness considered for both types of ribs, helical and circumferential, was 6 mm and rib intersections were materialized by means of an offset to avoid local over thickness. This is, circumferential ribs were slightly displaced with respect to helical rib intersections, as it can be seen in Figure 4. In the same figure, the geometry and large-scaled dimensions of the cylindrical lattice technology demonstrator considered in the second step of the virtual testing procedure can be observed. In this case, the load introduction interfaces reinforcing both extremes of the specimen are also included. These interfaces were made with steps of quasi-isotropic $(45,0,-45,90)_s$ laminates of the same material as in the lattice ribs. Observe that the final dimensions of the cylindrical lattice structure in Figure 4 are slightly different from the dimensions considered in the first stage of the procedure.

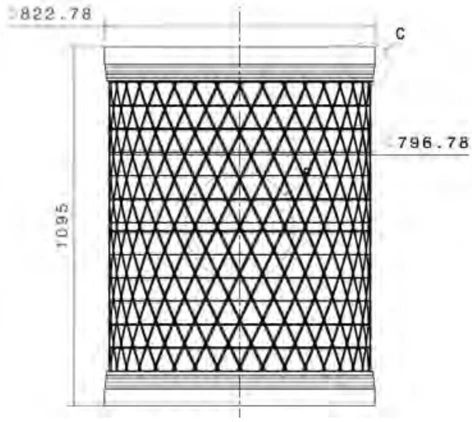

Figure 4. Geometry of the cylindrical lattice structure considered in the virtual testing (Dimensions in mm) (ECE).

This second step in the virtual testing procedure of the technology demonstrator was carried out through two modeling techniques. The global response was assessed with a simpler model that combined shell elements in the load interfaces of the structure with beam elements in the lattice part of the structure. The local failure of the structure was analyzed by means of a more complicated model using solid elements to model the structure. On one hand, solid elements permitted calculating the out-of-plane stress and shear, which are necessary to calculate the failure index of the structure and for the use of cohesive elements to simulate the adhesive failure between the lattice part and the load interface elements. On the other hand, a complete model of the structure with a refined enough solid mesh was out of a reasonable computational capacity. For this reason, it was necessary to apply symmetries in the solid elements model. As a consequence, this model was not suitable for the frequency analysis and it could not perceive anti-symmetric buckling modes. In front of these limitations, studying the global response of the structure through a beam elements model was seen as a proper solution.

a. Beam FE model: Global response

The beam FE model developed was used for providing information about global structural performance. Although offset in the ribs intersection is modeled, these were assumed ideal and without material over-thickness. The structure was modeled using *B31* beams elements, while the interfaces were modeled with *S4* shell elements, as shown in Figure 5. The loading interfaces were modeled using shell elements and not solid elements because it is a suitable trade-off between accurate results and computational time for a global response assessment. The shell surfaces were placed inside and outside the beam elements simulating the lattice, without any direct contact between nodes. Tie constraints were used to impose the same DOF between the shell surfaces and the beams. The outer surface was the master surface with a relation node to node to the inner shell surface and the beam elements. The surfaces were separated in sets of elements for each step of the interface and the laminate lay-up was defined independently for each set.

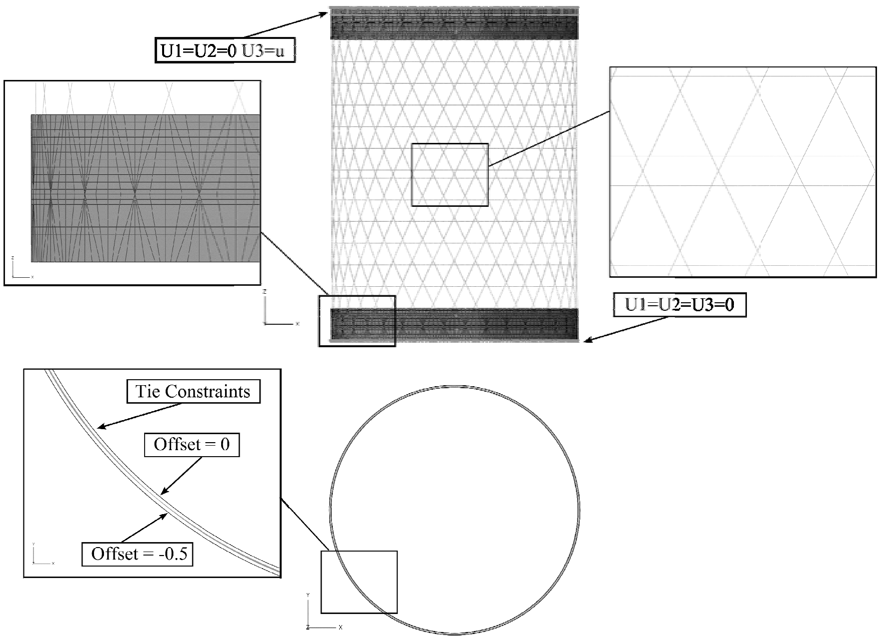

Figure 5. Virtual Testing: Beam FE model for global response: buckling conditions.

The frequency analysis was carried out clamping the lower extreme, while in the upper extreme a coupling constraint was applied to the mass point representing the satellite s/c. The conditions considered to simulate the satellite were the same as the ones that will be used in the experimental test, where the satellite s/c will be replaced for an element with the characteristics summarized in Table 4. The idea was to use the experimental results to validate the FE results and, afterwards, extrapolate these results to the real satellite in-work conditions (Table 3).

Table 4. Assumed satellite conditions for the laboratory frequency test.

Mass [kg]	CoG [mm]	Ixx [kg·m^2]	Iyy,Izz [kg·m^2]
200	0	140	300

The buckling analysis was carried out with the aim of estimating the approximate the buckling load of the structure, although its failure was expected before geometric non-linearities could cause any important destabilization. In the simulations, a compressive displacement of 5 mm was applied to the upper extreme of the cylinder, while the linear DOF of the nodes of the lower extreme were constrained (U1 = U2 = U3 = 0).

b. Solid FE Model: Local Submodeling

The cylindrical lattice technology demonstrator was modeled with *C3D8* solid elements for a more accurate analysis in combination with the node-based submodeling technique. The global model provided the displacements to the local submodel which assessed the failure criteria. In order to reduce the computation size and time of the global model, symmetries were applied in the three orthogonal planes and obtaining an eighth part of the structure. Although, failure was expected before reaching the buckling load, a non-linear analysis was applied.

Two local models were created, one for studying the section discontinuity around the end of the interface (Submodel A) and the other to study a rib intersection far from the extremes (Submodel B). A view of the global model plus the two submodels can be seen in Figure 6.

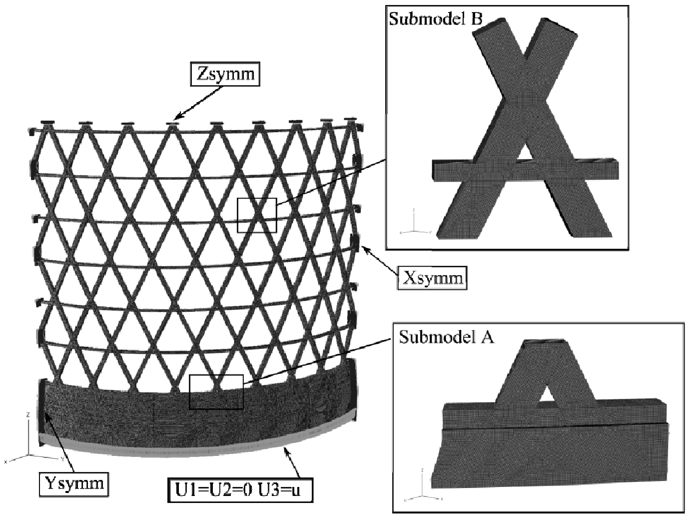

Figure 6. Virtual Testing: Solid global and local FE models for failure analysis.

In order to overcome the uncertainty about the exact geometry of the rib intersections and with the aim of modeling simplification, an engineering solution was used. On the one hand, the rib intersections were modeled with the same thickness as ribs. On the other hand, the material properties in terms of stiffness were increased with respect to those of the ribs by a 1.75 factor in order to take into account the accumulation of material. In the global model equivalent laminate properties were calculated for the rib intersections, while in the local model each layer was defined using a laminate solid section.

Intralaminar failure was assessed using LaRC-04 failure criteria (Camanho, 2006) with a UVARM user routine. These failure criteria are based on the different failure mechanisms of composite materials and take into consideration both non-linear shear behavior and in-situ effects. LaRC-04 is not a damage model and, consequently, it is only suitable to detect failure onset. In the present report, as the objective was assessing the final structural load, the collapse for intralaminar failure of the structure was established when 50% of the section of the rib is damaged. LaRC-04 failure criteria were applied to both local models. For this analysis, a perfect adhesive union was supposed in the interfaces (Submodel A). The material strength properties considered in the failure analysis of the cylindrical lattice structure are summarized in Table 5. Apart from the usual strength properties, LaRC-04 specific parameters are also included (see Camanho (2006) for further reference).

Table 5. Mechanical properties of the Epoxy/M40J UD CFRP for LaRC-04 failure criteria. (*X* and *Y* are the longitudinal and transverse strengths, S_L is the shear strength, α_0 is the fracture angle, β is the shear response factor, *g* is the toughness ratio (G_I/G_{II}), S_{IS} in situ shear strength).

X_T (MPa)	X_C (MPa)	Y_T (MPa)	Y_C (MPa)	S_L (MPa)	α_0 (°)	β	g	S_{IS} (MPa)
1345	653	40	183	66	53	2.44e-8	0.5	78

The possible adhesive peel-off between the ribs and interfaces was studied following the procedure developed in (Camanho, 2011a; Camanho, 2011b). First, the critical zones were established using Ye's criterion (Ye, 1988), which was also implemented in a UVARM user routine. Ye's criterion is suitable for a qualitatively analysis of delamination or peel-off. However, as a stress criterion, it is not useful for assessing the delamination load because it is mesh-dependent. A view of the peel-off predictions after Ye's criterion is shown in Figure 7(A). The second stage consisted in a Virtual Crack Closure Technique (VCCT) analysis, which is available in Abaqus v6.9. As VCCT analysis needs an initial pre-crack, which is recommended to be the minimum detectable defect, an initial pre-crack or peel-off area of 1 × 0.3 mm was created in the most critical zone after Ye's criterion. A detail of the pre-crack created in the local model for the VCCT analysis can be seen in Figure 7(B).

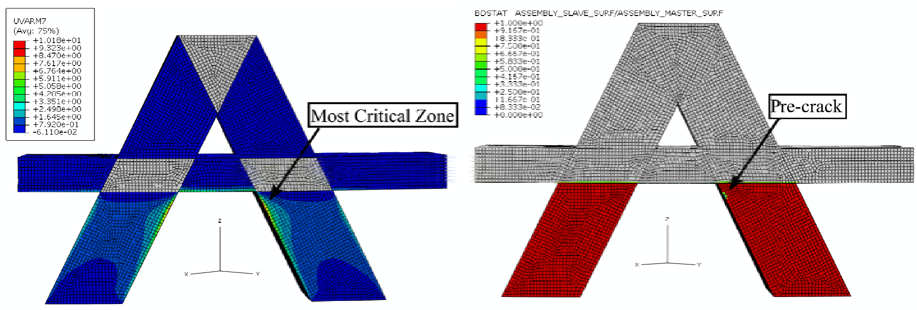

(A) (B)

Figure 7. Simulation of the adhesive peel-off in the local submodel: (A) Predictions of the Ye's criterion and (B) Initial pre-crack for the VCCT analysis.

Additionally, the adhesive peel-off between the ribs and load interfaces was also analyzed by means of cohesive elements involving a non-linear analysis and requiring the extra parameters reported in Table 6 to describe the constitutive material behavior of the adhesive. A cohesive layer of 0.01 mm was created between the external rib surfaces and the loading interface with Abaqus *COH3D8* elements. In this case, not pre-crack was considered.

Table 6. Adhesive facture properties.

G_{Ic} (J/mm^2)	G_{IIc} (J/mm^2)	S_{Ic} *(MPa)*	S_{IIc} *(MPa)*	η mix mode
0.6	2.1	40	75	2

4. Results and discussion

The results of the parametric analysis were summarized in a set of figures showing the dependencies between the design variables and the cylinder behavior. These figures and results allowed the determination of the most suitable lattice configuration in terms of natural frequencies, buckling load and low mass imposed at the beginning of the process. As mentioned before, this solution was found to be the configuration given by a cylindrical lattice with 36 helical ribs and 14 circumferential ribs and a rib thickness of 6 mm. Here, for conciseness reasons, only the results of the second step in the virtual testing of the technology demonstrator are presented.

1. Beam FE model results

The frequency analysis provided the specimen natural frequencies for the dynamic test conditions previously specified. Table 7 includes the obtained natural frequencies obtained organized in function of the evaluated stiffness. The deformed shapes of the structure corresponding to these natural frequencies are reported in Figure 8. All the reported frequencies met the imposed design conditions for the cylindrical lattice structure.

Table 7. Cylindrical lattice natural frequencies predicted with the virtual analysis.

1st Lateral Freq. [Hz]	Torsion Freq. [Hz]	2nd Lateral Freq. [Hz]	Axial Freq. [Hz]
41.5	51.7	81.6	203.4

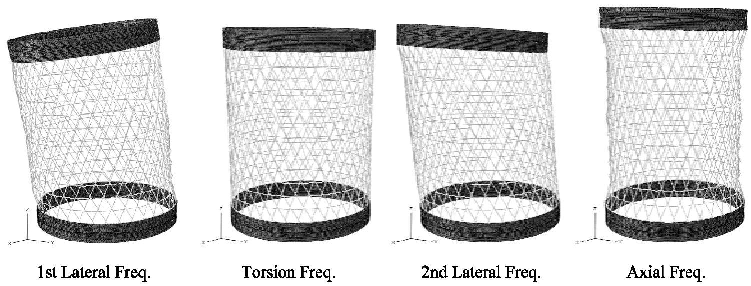

Figure 8. Deformed shapes of the lattice corresponding to the natural frequencies.

The buckling analysis found a multitude of buckling modes (eigenvectors) with a similar eigenvalue. Therefore, it did not exist a predominant buckling mode and a small variation in geometry, material properties or load conditions can bring to one or other buckling mode. The critical buckling load was calculated with the eigenvalues and the stiffness obtained in a linear analysis and are summarized in Table 8. The deformed shapes of the structure corresponding to the first three buckling modes are shown in Figure 9.

Table 8. Buckling loads corresponding to the first three buckling modes.

Buckling Mode	First	Second	Third
Buckling Load [kN]	1095.2	1118.8	1123.6

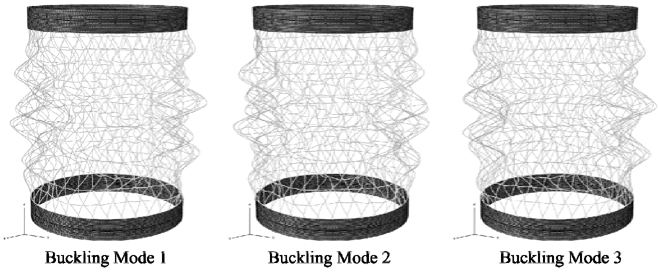

Figure 9. Deformed shapes of the cylindrical lattice corresponding to the first three buckling modes.

2. Solid FE model results

The load versus displacement curve and the associated stiffness assessed with the global model for the cylindrical lattice structure for linear and non-linear analyses are shown in Figure 10. In the figure, the reported displacement is the displacement of the upper extreme of the structure while the reported load corresponds to the reaction force assessed in the lower extreme. The figure also includes the failure loads predicted for each failure mechanism with the local submodels. Only the LaRC-04 predictions for the intralaminar failure of the fiber in compression are included in the figure as this are the most critical.

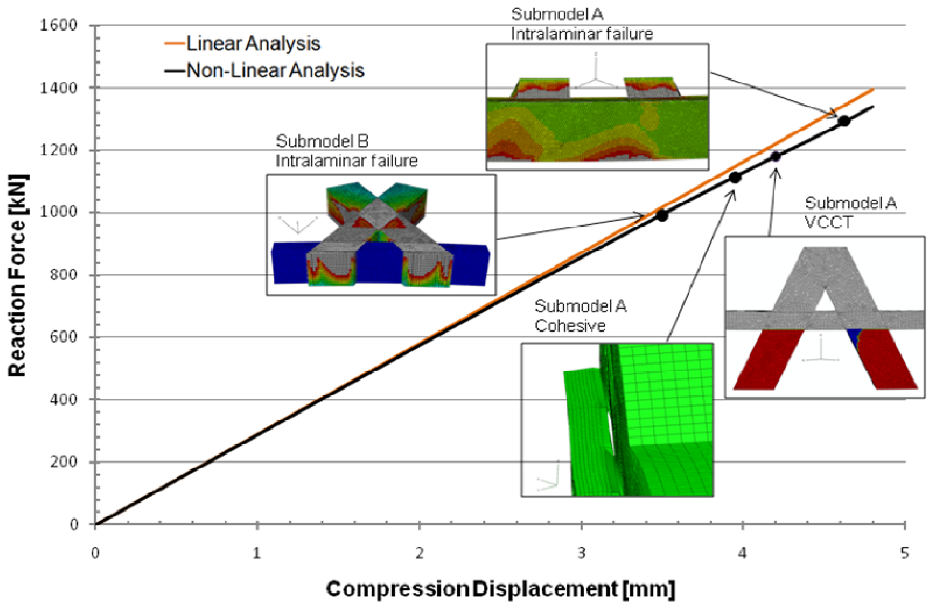

Figure 10. Load versus displacement curve predicted with the global FE model with linear and non-linear and failure predictions of the local submodels (intralaminar failure corresponds to compressive fiber compression).

The load versus displacement curves obtained with linear and non-linear analyses are common until the critical buckling load (Figure 10). Since, specimen collapse is predicted before the buckling load and the rest of failure modes are indicative because any damage model is applied; linear analysis is shown as a proper approach in terms of computationally efficiency.

The failure loads calculated with the local submodels are included in Table 9. The failure for adhesive peel-off calculated with cohesive elements is approximate as cohesive elements do not provide information about the exact moment when debonding takes place.

Table 9. Failure load for each failure mode calculated with local submodels.

Local model	Failure mechanism	Failure Load [kN]
Submodel A: Intersection near interfaces	Intralaminar failure	1290
	Adhesive peel-off (VCCT)	1180
	Adhesive peel-off (Cohesive)	1112
Submodel B: Intersection remote form interfaces	Intralaminar failure	991

Comparing the results predicted for buckling loads, intralaminar failure and adhesive peel-off between the lattice ribs and the load interfaces of the structure, it can be observed that according to the virtual testing procedure the cylindrical lattice structure is envisaged to fail by the collapse of the ribs near a rib intersection in the central area of the lattice. Actually, this failure is predicted at a compressive load of about 991 kN by longitudinal fiber compression. This failure of the structure is previewed at a lower load than the critical load corresponding to the first buckling, which was the desired response of the structure. The rest of the failure modes considered by the local submodels are predicted after the collapse of the structure by fiber compression and buckling. This result confirmed the important load capacity of the lattice structure and its suitability as a structural load-carrying element for aerospace application.

5. Conclusions

A virtual testing procedure for designing composite cylindrical lattice structures for aerospace applications has been presented. In a first design stage a parametric analysis of a preliminary model was used as a decision tool to determine the best lattice configuration in terms of natural frequencies, buckling loads and element weight. The second was devoted to the analysis of the technology demonstrator test in order to predict the mechanical behavior of the real structure. The global structural performance in terms of natural frequencies and buckling modes was studied with a FE model combining beam elements for the lattice part and shell elements for the loading interfaces. Failure was investigated with complete FE solid elements through the submodeling technique. The global model was used to obtain the global response of the structure while more refined local models were used to investigate the intralaminar failure and adhesive peel-off between ribs and load interface in the load interface areas and intralaminar failure in the lattice area. The LaRC-04 failure criteria were used by means of user subroutines for the analysis of the intralaminar failure. The adhesive peel-off between load interfaces and lattice ribs was studied with a methodology including Ye’s qualitative criterion, VCCT and cohesive elements.

The results of the virtual testing procedure of the composite cylindrical lattice determined the failure of the structure at a compressive load of about 991 kN demonstrating the load capacity of the cylindrical lattice structure. This failure was predicted to correspond to fiber compressive failure in the ribs of the lattice part far from the load interfaces.

Finally, the virtual test procedure allowed finding the best solution in different aspects for the design of a composite cylindrical lattice structure for aerospace applications. The lattice technology demonstrator was manufactured by ECE with a Viper-6000 Fiber Placement System developed by Cincinnati Machine. The layering process was automated using CNC technology based on the ACES® programming system. After the layering process, the lattice specimen was vacuum bagged and cured in an autoclave following the recommendations of the material’s manufacturer. As no triangular expansion tools were used during the curing process, rib intersections were not constrained and the final geometry of the ribs was not rectangular in their cross-section but dome-shaped. With the aim of simplification, this fact was not taken into account in the FE simulations. Moreover, at this stage of the project the effects of the curing process were not taken into account although they are deemed to be significant. Further investigation of these effects on the final response of the structure is planned and the updated results will be the object of a future report. Once available, the results of the experimental tests carried out with this technology demonstrator will allow the validation of the virtual test procedure and will be reported in future communications.

6. References

1. Bunakov, V.A., “Design of axially compressed composite cylindrical shells with lattice stiffeners”. Optimal Design – Theory and applications to materials and structures, Edited by Vasiliev, V.V. and Gürdal, Z., pp. 207-246, 1999
2. Cagdas, I. U., “Assessment of the accuracy of homogenization in finite element analysis of grid plates under transverse loads”. Engineering Computations: International Journal for Computer-Aided Engineering and Software, vol. 27, pp. 676-693, 2009
3. Camanho, P.P., Turon, A., Sarrado, C., Guillamet G., Trias, D., Simulation of delamination in polymer composites: best practices at different levels of analysis. Technical Interchange Meeting (TIM) on Fracture Control of Spacecraft, Launchers and their Payloads and Experiments, ESA/ ESTEC March 23-24 2011.
4. Camanho, P.P, Turon A., Lopes, C.S., Trias, D., TN410: Best Practice. Analysis Methods, DELAT project. February 2011.
5. Higgins, J.P.E, Wegner, P., Viisoreanu, Adrian. and Sanford, G., “Design and testing of the Minotaur advanced grid-stiffened fairing”, Composite Structures, vol. 66, pp. 339-349, 2004.
6. Higgins, J.P.E and Van West, B.P., “NDE and repair of damaged Minotaur fairing shell”, Composite Structures, vol. 67, pp. 189-195, 2005.
7. Higgins, J.P.E, Wegner, P., Van West, B. P. and Viisoreanu, Adrian., “Post-buckling test response and analysis of fiber composite grid-stiffened structures”, American Institute of Aeronautics and Astronautics, vol. 1332, 2002
8. Huybrechts, S. and Meink, T.E., “Advanced grid stiffened structures for the next generation of launch vehicles”, IEEE Aerospace Conference Proceedings. , vol. 1, pp. 263-270, 1997
9. ICARO Project Team, Vilanova, J., del Olmo, E., “Stiffened Monolithic Structures. Vega Payload Adaptor Enhancement. Trade-off study: Monolithic, Grid & Lattice Designs (Activity 3.3)”. EADS CASA Espacio. Report ECE-ICA-RPT-0006_01_0, 2010
10. Morozov, E.V., Lopatin, A.V., Nesterov, V.A., “Finite-element modeling and buckling analysis of anisogrid composite lattice cylindrical shells”. Composite Structures, vol. 93, pp. 308-323, 2011
11. Mountain, J., “FE based design of A-6 inner upper wing panels using anisogrid lattice concept”. Engineering School of the Cranfield University (UK), 2007
12. Totaro, G. and Gurdal, Z., “Optimal design of composite lattice shell structures for aerospace applications”. Aerospace Science and Technology, vol. 13, pp. 157-164, 2009
13. Vasiliev, V.V., Barynin, V.A. and Rasin, A.F., “Anisogrid lattice structures –survey of development and application”, Composite Structures, Vol. 54, pp. 361-370, 2001
14. Vasiliev, V.V. and Razin, A.F., Anisogrid composite lattice structures for spacecraft and aircraft applications”. Composite Structures, Vol. 76, pp. 182-189, 2006
15. Vasiliev, V.V. and Morozov, E.V., “Advanced mechanics of composite structures”. Editey by Washigton: Taylor and Francis, pp. 470-480, 2007
16. Wegner, P., Higgins, J.P.E and Van West, B.P., “Application of advanced grid-stiffened structures technology to the minotaur payload fairing”, American Institute of Aeronautics and Astronautics, vol. 1336, 2002

17. Ye, L., “Role of matrix resin in delamination onset and growth in composite laminates”, Composites Science and Technology, 33 (4), pp. 257-277, 1988

7. Acknowledgment

This study has been funded by CDTI (Spain) within the frame of the CENIT-ICARO program where University of Girona collaborates with EADS CASA Espacio (ECE). The first author acknowledges the PhD scholarship BES-2010-036295 funded by the Spanish Government in the VLANCO project (MAT2009-07918).